Transport of solar wind into Earth's magnetosphere through rolled-up Kelvin–Helmholtz vortices

H. Hasegawa[1], M. Fujimoto[2], T.-D. Phan[3], H. Rème[4], A. Balogh[5], M. W. Dunlop[6], C. Hashimoto[2] & R. TanDokoro[2]

[1]*Thayer School of Engineering, Dartmouth College, Hanover, New Hampshire 03755-8000, USA*
[2]*Department of Earth and Planetary Sciences, Tokyo Institute of Technology, Meguro, Tokyo 152-8551, Japan*
[3]*Space Sciences Laboratory, University of California, Berkeley, California 94720-7540, USA*
[4]*Centre d'Etude Spatiale des Rayonnements, BP 4346, Toulouse 31029, France*
[5]*Space and Atmospheric Physics Group, Imperial College, London SW7 2BZ, UK*
[6]*Space Sciences Division, Rutherford Appleton Laboratory, Chilton, Didcot, Oxfordshire OX11 0QX, UK*

Establishing the mechanisms by which the solar wind enters Earth's magnetosphere is one of the biggest goals of magnetospheric physics, as it forms the basis of space weather phenomena such as magnetic storms and aurorae[1]. It is generally believed that magnetic reconnection is the dominant process, especially during southward solar-wind magnetic field conditions when the solar-wind and geomagnetic fields are antiparallel at the low-latitude magnetopause[2]. But the plasma content in the outer magnetosphere increases during northward solar-wind magnetic field conditions[3,4], contrary to expectation if reconnection is dominant. Here we show that during northward solar-wind magnetic field conditions—in the absence of active reconnection at low latitudes—there is a solar-wind transport mechanism associated with the nonlinear phase of the Kelvin–Helmholtz instability[5]. This can supply plasma sources for various space weather phenomena.

Along the outer boundary of Earth's magnetosphere, there is a boundary layer that contains plasma of dominantly solar-wind origin[6] (Fig. 1a). The boundary layer exists for all orientations of the solar-wind magnetic field, but it tends to be thicker when the solar-wind field points northward[3,4]. The existence of the boundary layer implies penetration of solar wind across the magnetopause. Although reconnection between solar-wind and terrestrial magnetic fields can readily account for solar-wind entry during southward solar-wind magnetic field conditions, it is at present not known how the plasma crosses the magnetopause when the solar-wind magnetic field is oriented northward and parallel to geomagnetic fields and reconnection is less efficient, although there is a suggestion that simultaneous northern and southern cusp reconnection could result in the formation of the boundary layer at low latitudes[7]. Several candidate local entry mechanisms unrelated to reconnection have been proposed[8], one of which is the Kelvin–Helmholtz instability (KHI) that could occur along the flanks of the magnetosphere where the shocked solar wind is flowing fast relative to the stagnant magnetospheric plasma[9,10] (Fig. 1). Recent numerical simulation models[11–16] suggest that fast plasma transport across the magnetopause can be accomplished by the KHI only when the KHI has grown sufficiently to form rolled-up vortices that can engulf plasmas from both sides of the magnetopause. In these models, the collapse of, or reconnection within, such a vortex (in the nonlinear phase of the KHI) is responsible for the plasma transport.

Multiple and quasi-periodic encounters by spacecraft with the magnetopause and vortex-like flow perturbations near the magnetopause have been reported, and are often interpreted as representing surface waves or vortices excited by the KHI[17–21]. But as long as these signatures are observed only by a single spacecraft, one cannot tell unambiguously whether the KHI has reached its nonlinear stage and is generating rolled-up vortices, which are the crucial ingredient for plasma transport, or if they are just ripples or small-amplitude Kelvin–Helmholtz (KH) vortices on the magnetopause surface. The KH rolled-up vortex expected to form at the magnetopause has complex structures, such as vortical plasma flow and a filament-like high density region intruding into the low density (magnetospheric) region (see Fig. 1). To resolve such complex structures in the KH vortices, multipoint *in situ* measurements as carried out by the Cluster mission are essential, as is comparison with realistic three-dimensional (3D) plasma simulations.

Here we report multi-spacecraft measurements that provide unambiguous evidence for rolled-up vortices at the flank magnetopause as well as simultaneously observed boundary-layer characteristics that result from plasma transport across the boundary, such as would be expected from the suggested KHI mechanism.

The four Cluster spacecraft forming a tetrahedron made a

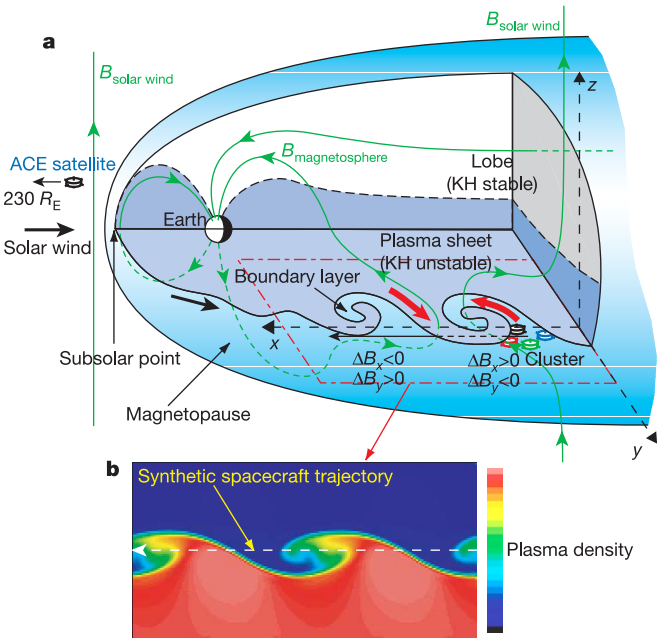

Figure 1 Three-dimensional (3D) cutaway view of Earth's magnetosphere, showing signatures of Kelvin–Helmholtz instability (KHI). **a**, View of the magnetosphere, showing the KH vortices at the duskside magnetopause. The velocity gradient across the magnetopause increases with distance from the subsolar point. The KHI occurs at the interface between the solar wind and the plasma sheet because the plasma energy dominates in both regions, whereas it does not occur at the surface of the lobes where the magnetic energy dominates and the magnetic tension prevents it from deforming the magnetopause. Consequently, the KH vortices evolve only along the low-latitude magnetopause and only low-latitude portions of the magnetospheric and solar-wind field lines are entrained into the vortices, inducing characteristic field perturbations in regions off the equatorial plane where the Cluster spacecraft were located. The satellites were situated at $(x, y, z) \approx (-3, 19, -3)$ Earth radii (R_E) in GSM (geocentric solar magnetospheric) coordinates, and were separated by ~2,000 km from each other. The coordinate system in the figures is defined such that $-x$ is in the direction of motion of the vortex structure which was sliding anti-sunward in the spacecraft frame, y points outward along the magnetopause normal, and z points to the north. **b**, Vortex structure resulting from a 3D numerical simulation of the magnetohydrodynamic KHI under a magnetosphere-like geometry, with the plasma sheet sandwiched between the two lobes. Colour-coded is the plasma density (minimum, 0 cm^{-3}; maximum, 5.0 cm^{-3}) in an x-y cross-section cut below the equatorial plane. The density, velocity and magnetic field variations expected when a synthetic satellite passes through the centre of the KH vortices to the left are shown in Fig. 2.

fortuitous direct encounter with the rolled-up vortices (Fig. 2) on 20 November 2001 when the upstream solar-wind magnetic field observed by the ACE spacecraft pointed northward, that is, when reconnection was less efficient but the condition was favourable for the KHI[22] at the low-latitude magnetopause. The solar-wind and magnetospheric magnetic fields on the dusk flank magnetopause were approximately parallel throughout the 16 min interval (Fig. 2f, g). The period of the vortices encounter was embedded in a more than 13-h interval of quasi-periodic plasma and magnetic field perturbations related to deformations of the magnetopause (09:30–23:30 UT). Rolled-up vortices were identified far more clearly by taking full advantage of multi-spacecraft information (Fig. 2e). The flow vectors, transformed into the frame of the vortices and viewed from the north, rotate anticlockwise around the centre of the vortices (marked by the red vertical lines in Fig. 2), as expected at the duskside magnetopause. Near these vortices, the density observed by the Cluster 1 spacecraft (C1) located farthest from the magnetopause (marked by the blue arrows in Fig. 2b) toward the magnetosphere was often higher than that observed by C3 or C4 (Fig. 2c, d). These instances of higher density at C1 are marked by red bars in Fig. 2c. Such high density regions appear to be connected to the dense solar wind on the anti-sunward side, for example, at 20:27:30 UT in Fig. 2d, rather than detached from the solar-wind region. This feature is consistent with the simulation result (Fig. 1b), and indicates that the dense regions result from the roll-up of the solar-wind plasma associated with the growth of the KHI (Fig. 1b), not from the impulsive penetration process[23]. The density variation observed by C1 (Fig. 2c) is similar to that expected when a synthetic spacecraft moves through the central portion of the simulated vortex and crosses the magnetopause back and forth (Fig. 1b), suggesting that C1 was in the vicinity of the centre of the vortices.

In addition to the density and flow signatures of the rolled-up KH vortices, we identified a unique magnetic field perturbation pattern associated with these vortices, which should appear only in a 3D configuration of the magnetosphere where the KH-unstable plasma sheet is sandwiched between the KH-stable northern and southern lobes (Fig. 1a). A numerical simulation of the KHI that considers this 3D magnetosphere-like geometry predicts that this field perturbation manifests in boundary regions between the plasma sheet and the lobes. This is because only low-latitude portions of the field lines surrounding the magnetopause are engulfed into the vortices, while those at high latitudes are unaffected (see Fig. 1 legend). Figure 2f shows that magnetic field perturbations seen in the high density (solar-wind) region ($\Delta B_x > 0$ and $\Delta B_y < 0$) and in the low density (magnetospheric) region ($\Delta B_x < 0$ and $\Delta B_y > 0$) have polarities in precise agreement with the 3D KHI effect on the magnetic field on the southward side of the equatorial plane where Cluster resided (Fig. 1a). The combined plasma and magnetic field observations provide unambiguous identification of rolled-up

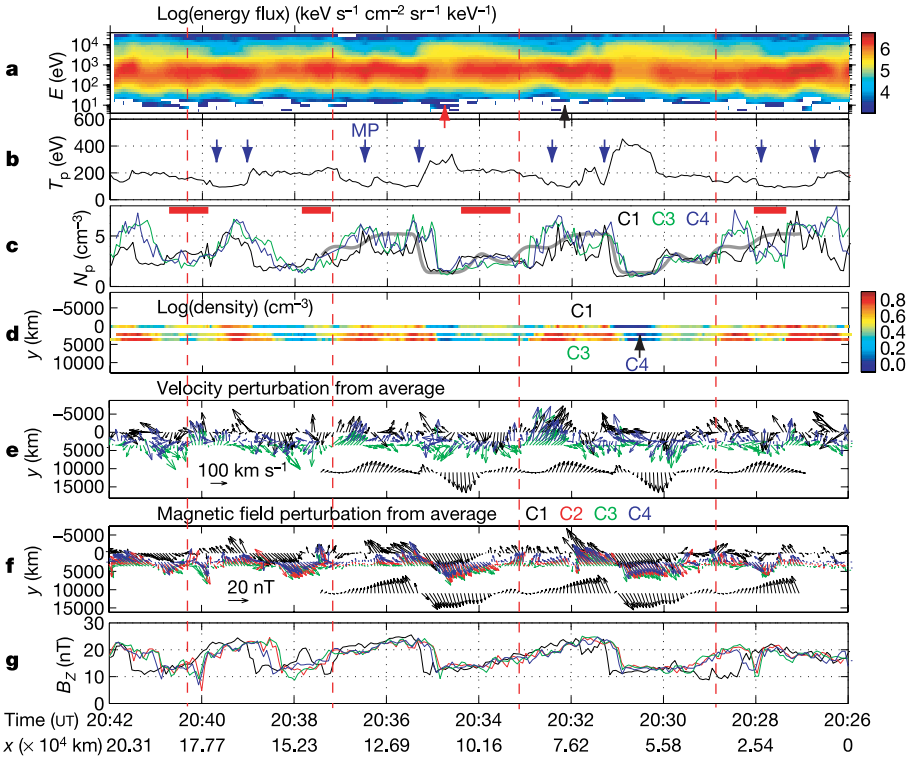

Figure 2 Detection by Cluster of rolled-up plasma vortices on 20 November 2001 (20:26–20:42 UT). **a**, The omni-directional energy spectrogram of ions observed by the Cluster 1 spacecraft (C1). Time progresses to the left, and is translated into the position of the spacecraft as follows. In Earth's rest frame, the spacecraft motion is neglected as compared to that of the vortices. $-x$ is in the direction of the vortex motion in the spacecraft frame. The vortex velocity, $\mathbf{V}_{mean}$, is computed by averaging over the above interval the ion bulk velocity vectors measured by C1, C3 and C4. The spacecraft position is determined using an equation, $x = |\mathbf{V}_{mean}|t + \Delta x_{i1}$, where t is time elapsed from the start of the interval, and Δx_{i1} is the x position of the ith spacecraft relative to C1. The arrows at the bottom denote the moments when the spectra and velocity distributions shown in Fig. 3 were observed. **b**, The ion temperature obtained by C1. The blue arrows mark approximate locations of the magnetopause. **c**, The plasma density variations are similar to those predicted by the numerical simulation (thick grey curve). Red bars indicate instances when C1 observed higher density than C3 and C4. **d**, The plasma density colour-coded and projected along the spacecraft trajectories. y is orthogonal to both x and the direction of the averaged magnetic field, $\mathbf{B}_{mean}$, and points outward along the magnetopause normal. **e**, **f**, The x–y projection of the velocity and magnetic field deviations from $\mathbf{V}_{mean}$ and $\mathbf{B}_{mean}$, respectively (C1,black; C2, red; C3, green; and C4, blue), along with the behaviour predicted by the simulation (below). The red dashed vertical lines mark the approximate centres of the vortices. The spacecraft separation distance and the length of the arrows are doubled in the y direction. **g**, The z component of the measured magnetic field.

vortices at the magnetopause, which, according to theory, is a key (and necessary) ingredient for plasma transport via KHI.

Evidence for plasma transport across the magnetopause was indeed observed. Cold solar-wind and hot magnetospheric ion populations are found to coexist in the vortices (Figs 2a, 3). Significant amounts of the solar-wind (<2 keV) and magnetospheric (>5 keV) ions were detected simultaneously in the same region on the magnetosphere side of the magnetopause. The appearance of rolled-up vortices in the vicinity of the boundary layer is strongly suggestive of the KHI mechanism for plasma transport across the boundary.

We could not deduce the exact microphysical process that leads to plasma transport within the KH vortices on the basis of the present measurements. However, we could rule out local reconnection, because during the interval of the vortex observations, we did not find signatures of plasma acceleration due to magnetic stresses[24,25] (see Supplementary Fig. 1) and D-shaped ion distributions characteristic of reconnection[26]. To exclude, conclusively, the possibility of remote (high-latitude) reconnection supplying the plasma observed at low latitude is more difficult. We do note, however, that the boundary layer ions, detected off the equator, were flowing poleward in precisely the same direction as the solar-wind flow. This seems inconsistent with the idea that high-latitude magnetopause reconnection[27], which would result in an equatorward flow at the observation point, produced the observed boundary layer. These observations thus indicate that reconnection occurred neither locally nor at the high-latitude magnetopause during the time of the observations of KH vortices. However, we cannot rule out the possibility that reconnection occurred in the past (but had ceased to exist) to produce a boundary layer which is now rolled-up by the KHI. Proving the existence of such a scenario is, however, even more difficult.

We estimate the speed of motion of the vortices by averaging over the vortices' interval the velocity values measured by the three spacecraft (C1, C3 and C4) on which the plasma instruments were operative. Time is then translated into distance of the spacecraft from a certain position in a vortex, and the length scale of one vortex is estimated to be 40,000–55,000 km (see Fig. 2). Consequently, the initial thickness of the velocity shear layer is inferred to have been roughly 5,000–7,000 km, because the wavelength of the fastest growing KH mode is approximately eight times the initial total thickness of the velocity shear layer[28]. According to numerical simulations, the width of the sufficiently developed KH vortex equivalent to that of the plasma boundary layer reaches about four times the initial thickness. We therefore infer that the boundary layer with the thickness of 20,000–28,000 km had been formed in the most KH-unstable low-latitude regions near, or at least further downstream of, the observation site.

The present results indicate that the KHI occurs at the flank magnetopause and that it may lead to solar-wind entry, perhaps via non-reconnection-associated processes, for northward solar-wind magnetic field. But the microphysical process that causes the plasma transport in the KH vortices, which would control the rate at which mass and energy of the solar wind are transferred, remain to be understood. The identification of the transport processes requires high-resolution measurements capable of resolving small-scale structures and dynamics embedded in the vortices. Such observations (which will be carried out by the future NASA Magnetospheric Multiscale mission[29] and the Japanese SCOPE mission) would enable us to determine the relative contributions of reconnection and the KHI during northward solar-wind magnetic field conditions. □

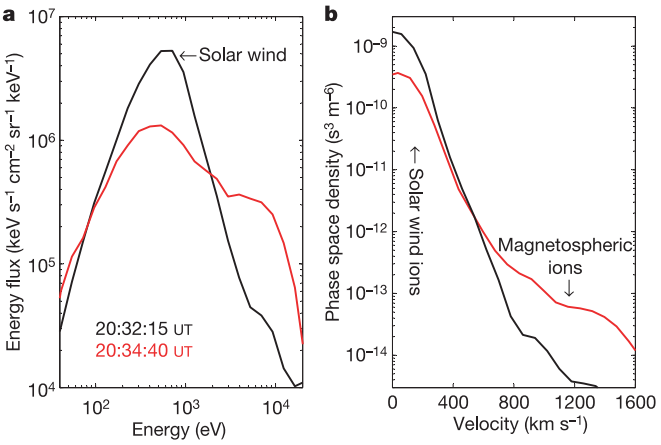

Figure 3 The ion energy spectra and velocity distributions observed by C1, showing the coexistence of the solar-wind (cold) and magnetospheric (hot) populations. The red curves were obtained at 20:34:40 UT when the spacecraft was in the magnetosphere near a vortex, while the black curves were obtained at 20:32:15 UT when the spacecraft was in the solar-wind-like region. **a**, The energy flux plotted as a function of energy in the spacecraft frame. The two peaks seen at 20:34:40 UT indicate the coexistence of two distinct populations. **b**, The velocity distributions at 90° to the magnetic field in the frame of bulk flow. The coexistence of solar-wind and magnetospheric ions in the vicinity of the vortices is suggestive of the KHI as a means of plasma transport across the magnetopause.

Received 12 April; accepted 29 June 2004; doi:10.1038/nature02799.

1. Akasofu, S.-I. Energy coupling between the solar wind and the magnetosphere. *Space Sci. Rev.* **28,** 121–190 (1981).
2. Cowley, S. W. H. in *Magnetic Reconnection in Space and Laboratory Plasmas* (ed. Hones, E. W.) 375–378 (Geophys. Monograph 30, American Geophysical Union, Washington DC, 1984).
3. Mitchell, D. G. *et al.* An extended study of the low-latitude boundary layer on the dawn and dusk flanks of the magnetosphere. *J. Geophys. Res.* **92,** 7394–7404 (1987).
4. Hasegawa, H., Fujimoto, M., Saito, Y. & Mukai, T. Dense and stagnant ions in the low-latitude boundary region under northward interplanetary magnetic field. *Geophys. Res. Lett.* **31,** L06802 (2004).
5. Chandrasekhar, S. *Hydrodynamic and Hydromagnetic Stability* (Oxford Univ. Press, New York, 1961).
6. Sckopke, N. G. *et al.* Structure of the low-latitude boundary layer. *J. Geophys. Res.* **86,** 2099–2110 (1981).
7. Song, P. & Russell, C. T. Model of the formation of the low-latitude boundary-layer for strongly northward interplanetary magnetic-field. *J. Geophys. Res.* **97,** 1411–1420 (1992).
8. Sibeck, D. G. *et al.* in *Magnetospheric Plasma Sources and Losses* Ch. 5 (ed. Hultqvist, B.) 207–283 (Space Sciences Series of ISSI 6, Kluwer Academic, Dordrecht, 1999).
9. Dungey, J. W. in *Proc. Ionosphere Conf.* 225 (Physical Society of London, 1955).
10. Miura, A. Anomalous transport by magnetohydrodynamic Kelvin-Helmholtz instabilities in the solar wind-magnetosphere interaction. *J. Geophys. Res.* **89,** 801–818 (1984).
11. Thomas, V. A. & Winske, D. Kinetic simulations of the Kelvin-Helmholtz instability at the magnetopause. *J. Geophys. Res.* **98,** 11425–11438 (1993).
12. Fujimoto, M. & Terasawa, T. Anomalous ion mixing within an MHD scale Kelvin-Helmholtz vortex. *J. Geophys. Res.* **99,** 8601–8613 (1994).
13. Huba, J. D. The Kelvin-Helmholtz instability: Finite Larmor radius magnetohydrodynamics. *Geophys. Res. Lett.* **23,** 2907–2910 (1996).
14. Nykyri, K. & Otto, A. Plasma transport at the magnetospheric boundary due to reconnection in Kelvin-Helmholtz vortices. *Geophys. Res. Lett.* **28,** 3565–3568 (2001).
15. Matsumoto, Y. & Hoshino, M. Onset of turbulence induced by a Kelvin-Helmholtz vortex. *Geophys. Res. Lett.* **31,** L02807 (2004).
16. Nakamura, T. K. M., Hayashi, D., Fujimoto, M. & Shinohara, I. Decay of MHD-scale Kelvin-Helmholtz vortices mediated by parasitic electron dynamics. *Phys. Rev. Lett.* **92,** 145001 (2004).
17. Ogilvie, K. W. & Fitzenreiter, R. J. The Kelvin-Helmholtz instability at the magnetopause and inner boundary layer surface. *J. Geophys. Res.* **94,** 15113–15123 (1989).
18. Kivelson, G. K. & Chen, S.-H. in *Physics of the Magnetopause* (eds Song, P., Sonnerup, B. U. Ö. & Thomsen, M. F.) 257–268 (Geophys. Monograph 90, American Geophysical Union, Washington DC, 1995).
19. Hones, E. W. Jr *et al.* Further determination of the characteristics of magnetospheric plasma vortices. *J. Geophys. Res.* **86,** 814–820 (1981).
20. Fairfield, D. H. *et al.* Geotail observations of the Kelvin-Helmholtz instability at the equatorial magnetotail boundary for parallel northward fields. *J. Geophys. Res.* **105,** 21159–21173 (2000).
21. Fujimoto, M., Tonooka, T. & Mukai, T. in *Earth's Low-latitude Boundary Layer* (eds Newell, P. T. & Onsager, T.) 241–251 (Geophys. Monograph 133, American Geophysical Union, Washington DC, 2003).
22. Miura, A. Dependence of the magnetopause Kelvin-Helmholtz instability on the orientation of the magnetosheath magnetic field. *Geophys. Res. Lett.* **22,** 2993–2996 (1995).
23. Lemaire, J. Impulsive penetration of filamentary plasma elements into magnetospheres of Earth and Jupiter. *Planet. Space Sci.* **25,** 887–890 (1977).
24. Paschmann, G. *et al.* Plasma acceleration at the Earth's magnetopause: Evidence for reconnection. *Nature* **282,** 243–246 (1979).
25. Phan, T.-D. *et al.* Extended magnetic reconnection at the Earth's magnetopause from detection of bi-directional jets. *Nature* **404,** 848–850 (2000).
26. Fuselier, S. A. in *Physics of the Magnetopause* (eds Song, P., Sonnerup, B. U. Ö. & Thomsen, M. F.) 181–187 (Geophys. Monograph 90, American Geophysical Union, Washington DC, 1995).

27. Kessel, R. L. *et al.* Evidence of high-latitude reconnection during northward IMF: Hawkeye observations. *Geophys. Res. Lett.* **23,** 583–586 (1996).
28. Miura, A. & Pritchett, P. L. Nonlocal stability analysis of the MHD Kelvin-Helmholtz instability in a compressible plasma. *J. Geophys. Res.* **87,** 7431–7444 (1982).
29. *Report of the NASA Science and Technology Definition Team for the Magnetospheric Multiscale (MMS) Mission* (NASA/TM-2000-209883, Goddard Space Flight Center, Greenbelt, MD, 1999).

Supplementary Information accompanies the paper on **www.nature.com/nature**.

Acknowledgements We are indebted to the Cluster team for the design and successful operation of the Cluster II mission. Part of this work was done while H.H. visited UC Berkeley.

Competing interests statement The authors declare that they have no competing financial interests.

Correspondence and requests for materials should be addressed to H.H. (hiroshi.hasegawa@dartmouth.edu).

Room-temperature ferroelectricity in strained $SrTiO_3$

J. H. Haeni[1], P. Irvin[2], W. Chang[3], R. Uecker[4], P. Reiche[4], Y. L. Li[1], S. Choudhury[1], W. Tian[5], M. E. Hawley[6], B. Craigo[7], A. K. Tagantsev[8], X. Q. Pan[5], S. K. Streiffer[9], L. Q. Chen[1], S. W. Kirchoefer[3], J. Levy[2] & D. G. Schlom[1]

[1]*Department of Materials Science and Engineering, Penn State University, University Park, Pennsylvania 16802-5005, USA*
[2]*Department of Physics and Astronomy, University of Pittsburgh, Pittsburgh, Pennsylvania 15260, USA*
[3]*Naval Research Laboratory, 4555 Overlook Avenue S.W., Washington DC 20375, USA*
[4]*Institute of Crystal Growth, Max-Born-Straβe 2, D-12489 Berlin, Germany*
[5]*Department of Materials Science & Engineering, University of Michigan, Ann Arbor, Michigan 48109-2136, USA*
[6]*Materials Science and Technology Division (MST-8), Los Alamos National Laboratory, Los Alamos, New Mexico 87545, USA*
[7]*Motorola Labs, 2100 East Elliot Road, Tempe, Arizona 85284, USA*
[8]*Laboratoire de Céramique, Ecole Polytechnique Fédérale de Lausanne, Lausanne CH 1015, Switzerland*
[9]*Materials Science Division, Argonne National Laboratory, Argonne, Illinois 60439, USA*

Systems with a ferroelectric to paraelectric transition in the vicinity of room temperature are useful for devices. Adjusting the ferroelectric transition temperature (T_c) is traditionally accomplished by chemical substitution—as in $Ba_xSr_{1-x}TiO_3$, the material widely investigated for microwave devices in which the dielectric constant (ϵ_r) at GHz frequencies is tuned by applying a quasi-static electric field[1,2]. Heterogeneity associated with chemical substitution in such films, however, can broaden this phase transition by hundreds of degrees[3], which is detrimental to tunability and microwave device performance. An alternative way to adjust T_c in ferroelectric films is strain[4–8]. Here we show that epitaxial strain from a newly developed substrate can be harnessed to increase T_c by hundreds of degrees and produce room-temperature ferroelectricity in strontium titanate, a material that is not normally ferroelectric at any temperature. This strain-induced enhancement in T_c is the largest ever reported. Spatially resolved images of the local polarization state reveal a uniformity that far exceeds films tailored by chemical substitution. The high ϵ_r at room temperature in these films (nearly 7,000 at 10 GHz) and its sharp dependence on electric field are promising for device applications[1,2].

Enormous strains can be imparted to thin films and have previously been used to alter the T_c of ferromagnetic[9,10] and superconducting[11–13] materials. For such phenomena, strain-induced enhancements in T_c as large as tens of degrees have been observed[9]. Owing to the strong coupling between strain and ferroelectricity, much larger T_c shifts are expected[4,6], and have been observed[7,8], in ferroelectric materials.

In its pure, unstressed form, strontium titanate ($SrTiO_3$) is an incipient ferroelectric. It remains paraelectric down to 0 K, although chemical[14,15] or isotopic substitution[16], as well as the application of stress[4], easily disturb this delicate state, resulting in ferroelectricity. The boundary conditions imposed by a substrate profoundly affect ferroelectricity in thin films. Figure 1 shows the predicted[4] shift in T_c for $SrTiO_3$ (ref. 17) under biaxial strain $\epsilon_s = (a_{\|}-a_0)/a_0$, where a_0 is the lattice parameter of free-standing $SrTiO_3$ and $a_{\|}$ is the in-plane lattice parameter of a biaxially strained (100) $SrTiO_3$ film. The hatched region shows the range in predicted T_c due to the spread in reported property coefficients for $SrTiO_3$ (refs 18, 19) that enter into the thermodynamic analysis. For example, for positive ϵ_s and $T > 120$ K, the enhancement in T_c is given by $\Delta T_c = 2\epsilon_s\epsilon_0 C(Q_{11}+Q_{12})/(s_{11}+s_{12})$, where ϵ_0 is the permittivity of free space, C is the Curie constant, Q_{11} and Q_{12} are the electrostrictive coefficients, and s_{11} and s_{12} are elastic compliances of $SrTiO_3$. The breadth of the hatched region in Fig. 1 for T_c is mainly due to the nearly factor-of-two variation in the ratio of $(Q_{11}+Q_{12})/(s_{11}+s_{12})$ for what are considered the most accurate reported values of these constants. These predictions imply that a biaxial tensile strain of order 1% will shift the T_c of $SrTiO_3$ to the vicinity of room temperature.

In practice, the synthesis of uniformly strained ferroelectric films is challenging. Epitaxial ferroelectric films are usually grown to thicknesses greatly exceeding their critical values, resulting in undesirable relaxation towards a zero-strain state by the introduction of dislocations. Dislocation densities of $\sim 10^{11}$ cm^{-2} are typical in epitaxial $Ba_xSr_{1-x}TiO_3$ films[20], and the resulting inhomogeneous strain further smears the phase transition, in addition to the effects of chemical heterogeneity mentioned above. Our approach to controlling the properties of ferroelectric $SrTiO_3$ films centres on the development of new substrates that enable the growth of uniformly strained films below, or at least far closer to, the critical thickness for relaxation.

Depending on the choice of substrate, films may be grown under compressive or tensile strain. Commercially available substrates that

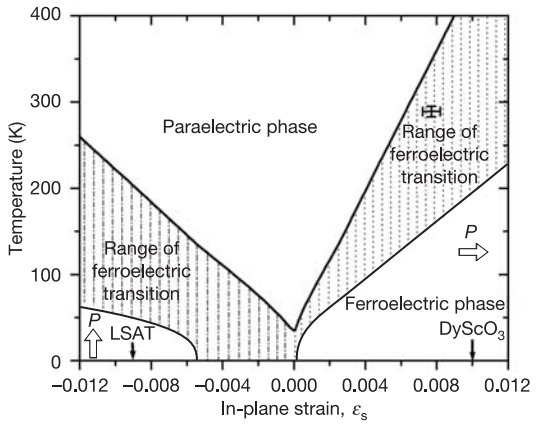

Figure 1 Expected shift in T_c of (100) $SrTiO_3$ with biaxial in-plane strain, based on thermodynamic analysis. The arrows indicate the predicted direction of the polarization for strained $SrTiO_3$: in-plane for biaxial tensile strain and out-of-plane for biaxial compressive strain. The ϵ_s values for $SrTiO_3$ fully constrained (commensurate) to the lattice constants of LSAT and (110) $DyScO_3$ substrates are indicated by the positions of the corresponding arrows. The cross shows the observed T_c shift of a 500-Å-thick $SrTiO_3$ film epitaxially grown on (110) $DyScO_3$.